De Rosario Martínez, H.; Page Del Pozo, AF.; Besa Gonzálvez, AJ.; Mata Amela, V.; Conejero Navarro, E. (2012). Kinematic description of soft tissue artifacts: quantifying rigid versus deformation components and their relation with bone motion. Medical & Biological Engineering & Computing. 50(11):1173-1181. https://doi.org/10.1007/s11517-012-0978-5

Kinematic description of soft tissue artifacts. Quantifying rigid vs deformation components and their relation with bone motion.

Helios de Rosario[*], Álvaro Page [#,Δ], Antonio Besa[†], Vicente Mata[†], Efraim Conejero*

[*]*Instituto de Biomecánica de Valencia, Universitat Politècnica de València, Edificio 9C, Camino de Vera s/n, E46022 Valencia, Spain*

[#]*Departamento de Física Aplicada. Universitat Politècnica de València, Camino de Vera s/n, E46022 Valencia, Spain.*

[Δ]*Grupo de Tecnología Sanitaria del IBV, CIBER de Bioingeniería, Biomateriales y Nanomedicina (CIBER-BBN).*

[†]*Departamento de Ingeniería Mecánica y de Materiales, Universitat Politècnica de València, Spain*

Corresponding Author:

Álvaro Page del Pozo

e-mail: afpage@ibv.upv.es

tel: +34963879160

fax: +34963879169

The total number of words of the manuscript, including entire text from title page to figure legends: **5005**

The number of words of the abstract: **198**

The number of figures: **6**

The number of tables: 1

ABSTRACT

This paper proposes a kinematic approach for describing soft tissue artifacts (STA) in human movement analysis. Artifacts are represented as the field of relative displacements of markers with respect to the bone. This field has two components: deformation component (symmetrical field) and rigid motion (skew-symmetric field). Only the skew-symmetric component propagates as an error to the joint variables, whereas the deformation component is filtered in the kinematic analysis process. Finally, a simple technique is proposed for analyzing the sources of variability in order to determine which part of the artifact may be modeled as an effect of the motion, and which part is due to other sources. This method has been applied to the analysis of the shank movement induced by a vertical vibration in 10 subjects. The results show that the cluster deformation is very small with respect to the rigid component. Moreover, both components show a strong relationship with the movement of the tibia. These results suggest that artifacts can be modeled effectively as a systematic relative rigid movement of the marker cluster with respect to the underlying bone. This may be useful for assessing the potential effectiveness of the usual strategies for compensating for STA.

Soft tissue artifacts, Human movement analysis, Kinematics, Vibrations, Systematic and random errors.

1. Introduction

Soft tissue artifacts (STA) are a major source of error in human movement analysis. Thus, there are many studies aimed at evaluating their nature and effects. Leardini et al. [17] reviewed different techniques for assessing and compensating for STA. More recently, Peters et al. [23] carried out a systematic review where they indicated the main limitations of published studies. As that review pointed out, the measurements of STA are varied, and such diversity complicates the comparison of results among studies.

Some studies have described STA as the displacement of individual markers in a bone-embedded reference frame, and have assessed specific anatomical landmark errors [27, 32], the distribution of artifacts depending on the segment region [28, 33], or local skin deformations [15].

Others have focused on the effects of STA on kinematic analysis, by comparing the results obtained from the measurements of skin markers with those obtained from an artifact-free gold standard. Such results are usually joint angles [3, 5, 18-19, 25], but some also compared the location of joint axes and centres of rotation [26, 31]. That approach is very useful for determining the expected size of STA errors for specific movements, although it does not provide us with information about the origin and characteristics of the artifacts themselves.

There have been some attempts to describe the kinematic nature of STA. It is widely acknowledged that STA cause a deformation of the marker cluster (DMC), plus a rigid movement (RM) of the whole set. The distinction between these components is actually the basis of some methods of STA assessment and compensation. Thus, the Point Cluster Technique evaluates these components through the variation in the inertia tensor of the marker cluster [2, 4, 6]: RM is characterized as the transformation of the eigenvectors, whereas DMC is calculated as the variation in the eigenvalues; alternatively, DMC has also been assessed as the variation in inter-marker distances [15]. However, there are few studies on the quantitative relationship between these components. Only recently, Stagni and Fantozzi [30] compared the values of RM and DMC for thigh and shank in order to evaluate the possible correlation between both components, and the possibility of compensating for STA on the basis of DMC information. That study suggested that deformations are not good indicators of the RM component.

The relation between STA and joint motion is also an important issue. STA result from motion, but they depend on different causes, including muscle deformations, skin sliding or inertial effects [17]. This diversity of mechanisms introduces potentially great variability. Although some studies suggest that the largest part of STA is systematic and associated with the movement cycle [25, 31], there is a shortage of published models that quantify such variability, or determine its effect upon the RM and DMC components of STA.

This study is aimed at answering two questions. First, what is the quantitative relationship between the RM and DMC components of STA? And second, are RM and DMC components essentially systematic, so that it would be possible to define functional relations with bone movement? The answers to these questions will be useful to assess the potential effectiveness of the usual strategies to compensate for STA.

To achieve this objective, a vector procedure to quantify and compare RM and DMC is proposed. This procedure provides us with information about both the movement of marker clusters as a single entity, and about individual markers as well. After separating both components, their variability is analyzed in order to determine what part is accounted for by the bone movement, and what part comes from other sources. This characterization is applied to the STA measured in an experiment, where the subjects' shanks were passively moved by vertical vibrations.

2. Methods

STA quantification approach

Let us consider a body segment whose position is measured from a cluster of n skin markers, P_i, and assume that we can observe the movement of the underlying bone by an artifact-free alternative method, like external fixators, intracortical pins or videofluoroscopy, as described in [23]. At the reference instant t_0, the bone is at pose B_0, and the skin marker cluster is at position P_{i0}, with their centroid in G_0 (Figure 1). In another instant, the bone moves from B_0 to B_1. This displacement can be described by the translation $\overrightarrow{\mathbf{G_0G_1}}$ plus a rotation that we

represent by the attitude vector $\vec{\boldsymbol{\theta}}$ [34]. These variables can easily be calculated from a set of bone points [21, 34].

If the markers were rigidly attached to the bone, then they would move from P_{i0} to a theoretical position P_{i1}. However, due to STA, skin markers may have moved with respect to the bone, and there may be some instrumental errors as well. Therefore, their observed position P_i will be different from P_{i1}.

The difference between P_{i1} and P_i ($\delta\vec{\mathbf{r}}_i'$ in Figure 1) is the position error of the markers, which is usually represented in a moving, bone-embedded anatomical frame, in order to describe the movement relative to the bone [9]. The same relative movement can be obtained from the calculations in any reference frame by applying to P_i the opposite displacement of the bone, $\left\{-\vec{\boldsymbol{\theta}},-\ \overrightarrow{\mathbf{G_0G_1}}\right\}$, so that they move to P_{i2}. The operation to perform such a finite displacement is [21]:

$$\overrightarrow{\mathbf{P_iP_{i2}}} = -\overrightarrow{\mathbf{G_0G_1}} - \sin\theta\ \ \vec{\mathbf{u}}\times\overrightarrow{\mathbf{G_1P_i}} + (1-\cos\theta)\ \vec{\mathbf{u}}\times\left(\vec{\mathbf{u}}\times\overrightarrow{\mathbf{G_1P_i}}\right) \qquad (1)$$

where $\vec{\mathbf{u}}$ is the unit vector of $\vec{\boldsymbol{\theta}}$.

Note that P_{i2} represents the position of the *i*-th marker affected by the STA, seen by an observer that moves as the bone does. Thus, the relative displacement of the marker with respect to the bone, as seen from a frame fixed to the bone, is:

$$\delta\vec{\mathbf{r}}_i = \overrightarrow{\mathbf{P_{i0}P_{i2}}} \qquad (2)$$

STA model: skew-symmetric and deformation fields

The error in the kinematic analysis is a rotation $d\vec{\boldsymbol{\theta}}$ and a translation $\overrightarrow{\mathbf{G_0G_2}}$, which results from fitting a rigid motion to the field of relative displacements, $\delta\vec{\mathbf{r}}_i$. For small rotations (<~10 deg), the fitted kinematic variables can be approximated by linear equations as in the analysis of infinitesimal displacements [20]:

$$d\vec{\boldsymbol{\theta}} \approx \overline{\overline{\mathbf{J}}}_{G0}^{-1}\sum_{i=1}^{n}\overrightarrow{\mathbf{G_0P_{i0}}}\times\delta\vec{\mathbf{r}}_i \qquad (3)$$

$$\overrightarrow{\mathbf{G_0G_2}} \approx \frac{\sum_{i=1}^{n}\delta\vec{\mathbf{r}}_i}{n} \qquad (4)$$

where $\overline{\overline{\mathbf{J}}}_{G0}$ is the inertia tensor of the marker set with respect to its centroid, assuming that the markers have unitary mass.

For small rotations, moreover, the RM component of the artifact can be approximated as a skew-symmetric field of displacements

$$\delta\vec{\mathbf{r}}_{si} = \overrightarrow{\mathbf{G_0G}_2} + d\vec{\boldsymbol{\theta}} \times \overrightarrow{\mathbf{G_0P}_{i0}} \qquad (5)$$

The DMC is just the remaining field $\delta\vec{\mathbf{r}}_{di}$, so that

$$\delta\vec{\mathbf{r}}_i = \delta\vec{\mathbf{r}}_{si} + \delta\vec{\mathbf{r}}_{di} \qquad (6)$$

Figure 2 shows a simulated example of the decomposition of a field of infinitesimal displacements into the RM and DMC components.

Most methods of motion analysis are based on rigid body kinematics, so that only the RM $(\delta\vec{\mathbf{r}}_{si})$ is compatible with the condition imposed by such models, and will propagate to the kinematic variables. On the other hand, DMC $(\delta\vec{\mathbf{r}}_{di})$ will have no effect on those calculations.

STA variability sources

STA depend on two main causes related to the motion: the slow compression and stretching of muscles, and the dynamic response of soft tissues to inertial forces in quick movements and impacts [24]. Both causes are systematic and only depend on the characteristics of the subject and the movement so, for identical repetitions of a movement, both RM and DMC should vary to some extent as a function of the bone motion, although some differences across repetitions can also be expected. The terms Phase-Dependent Variability (PDV) and Phase-Independent Variability (PIV) will be used to refer to the systematic variations of STA that only depend on the bone motion, and the remaining non-systematic variability, respectively. The size of both sources of variability may be evaluated as follows:

Let us consider a phase variable, called q, associated with the progression of a cyclic bone movement. For instance, q could be the hip flexion angle for the analysis of thigh movement during gait cycles. For a totally systematic relation between the STA and the bone movement (without PIV), there would be one single function $\delta\vec{\mathbf{r}}_i(\mathrm{q})$ that defines the STA exactly as a function of q for all cycles, and all the variability of this function would account for PDV. Due to the natural variability of the motion and uncontrolled factors, there is actually a

different function $\delta\vec{\mathbf{r}}_{ic}(\mathrm{q})$ for each cycle (c=1, 2, …, nc), although it can be related to a common average $\delta\vec{\mathbf{r}}_{i}(\mathrm{q})$, calculated as in [22]:

$$\delta\vec{\mathbf{r}}_{\mathrm{ic}}(\mathrm{q}) = \delta\vec{\mathbf{r}}_{\mathrm{i}}(\mathrm{q}) + \vec{\boldsymbol{\varepsilon}}_{\mathrm{ic}}(\mathrm{q}) \qquad (7)$$

where $\vec{\boldsymbol{\varepsilon}}_{\mathrm{ic}}(\mathrm{q})$ is an error function associated with non-systematic factors, and is the part that accounts for the PIV. The relative importance of PDV compared with PIV can be quantified by comparing the sums of squares associated with each function and the total variability. Thus, PIV may be quantified as the residual sum of squares, SSR:

$$SSR = \sum_{c=1}^{nc}\sum_{q\in Q}\left(\vec{\boldsymbol{\varepsilon}}_{\mathrm{ic}}(q)\right)^2 = \sum_{c=1}^{nc}\sum_{q\in Q}\left(\delta\vec{\mathbf{r}}_{ic}(q) - \delta\vec{\mathbf{r}}_{i}(q)\right)^2 \qquad (8)$$

The total variability of the STA (SST) can be calculated as:

$$SST = = \sum_{c=1}^{nc}\sum_{q\in Q}\left(\delta\vec{\mathbf{r}}_{ic}(q) - mean[\delta\vec{\mathbf{r}}_{i}(q)]\right)^2 \qquad (9)$$

where $mean[\delta\vec{\mathbf{r}}_{i}(q)]$ is the average of $\delta\vec{\mathbf{r}}_{\mathrm{i}}(\mathrm{q})$ across all the domain of q. Finally, PVD is quantified as the difference between the total and residual sums of squares:

$$SMM = SST - SSR \qquad (10)$$

This variability may be standardized as an *R*-value, the nonlinear correlation coefficient that is calculated from the variance ratio explained by the model:

$$R = \sqrt{\frac{SSM}{SST}} = \sqrt{1 - \frac{SSR}{SST}} \qquad (11)$$

This procedure can be applied to the whole position error of a marker, as in this example, or separately to the RM and DMC components. It can also be applied to the full set of markers in the cluster, by aggregating the sums of squares:

$$R = \sqrt{1 - \frac{\sum_{i=1}^{n} SSR}{\sum_{i=1}^{n} SST}} \qquad (12)$$

Experiment setup

With the purpose of illustrating the abovementioned characterization of STA, the artifacts caused by longitudinal vibrations applied to the shank were analyzed. The main objective of this experiment was the validation of the proposed description of STA from a mechanical point of view, rather than describing the actual artifacts that occur in common gestures.

The experiment was performed with 10 healthy volunteers (6 male and 4 female), aged between 18 and 51 years old. The procedure was approved by the IBV's ethical committee, and all subjects signed an informed consent prior to their participation.

Figure 3 shows the experimental device. The subjects sat on a fixed seat, and their left shank and foot were fitted onto a frame fixed onto an electro-dynamic vibration exciter (V712 Ling Dynamic Systems). Foot and tibia were fitted with a strap and side supports that exerted pressure on the foot insole, malleoli and femoral epycondiles. The top bar of the frame was adjusted and pressed down on the subject's knee to ensure that the tibia moved rigidly with the frame. Thus, it was possible to assess the artifact-free bone movement with a cluster of 8 markers attached to the frame. The skin movement was measured with a mesh of 14 reflective, circular markers of 10 mm diameter attached to the lateral side of the shank.

Prior to the experiment, the subjects were asked to try to move their leg in order to evaluate the relative motion of the bone with respect to the rigid frame. A set of two additional markers were placed on the anterior side of leg, over the tibia, at approximately 1/3 and 2/3 of the knee height. The pressure of the straps and supports was increased when the motions of those markers were larger than 1.0 mm in any direction. Considering that an average separation between those markers was around 200 mm, the error implied by that motion would be less than 1 mm in linear translations, and less than 0.6 deg (2/200 rad) in rotations.

In order to achieve perceptible STA, the subjects were asked to keep their legs relaxed, and before the trial a frequency sweep was performed between 5–15 Hz to detect the resonant frequency of each subject's shank. The resonant frequencies were between 9 and 13 Hz for all subjects.

After detecting the resonant frequency, a sinusoidal vibration at that frequency was applied to the device, with a peak-to-peak amplitude around 3 mm, and the motion of the frame and the skin markers was recorded. The motion transmitted to the leg was a linear translation without rotation, so the vertical displacement of the tibia was used as the phase variable *q*. The Kinescan-IBV videophotogrammetry system [20] was used for this purpose, with two cameras and a sampling frequency of 120 fps. The system was calibrated by bundle adjustment, and the instrumental error, assessed as in [20], was 0.3 mm in all coordinates.

Data processing and statistical analysis

The absolute movement of the frame/tibia was measured, and the artifact was calculated as described in the section "STA quantification approach". The size of $\delta\vec{\mathbf{r}}_i, \delta\vec{\mathbf{r}}_{di}, \delta\vec{\mathbf{r}}_{si}$, and the variables of the skew-symmetric field $\left\{d\vec{\boldsymbol{\theta}}\,; \overrightarrow{\mathbf{G_0G_2}}\right\}$ were assessed as their root mean square (RMS). These values were normalized with respect to the vibration amplitude in order to have comparable results in spite of departures from the nominal amplitude.

Finally, the relative importance of PDV and PIV were quantified by means of the *R* coefficient as defined in Eq. (11). In this experiment the tibia was rigidly attached to the vibrator by means of the rigid frame, and only experienced a vertical translation with no rotation. Therefore, the vertical displacement of the rigid frame was chosen as the variable q that described the cyclical motion. The R coefficient was calculated for $d\vec{\boldsymbol{\theta}}$ and $\overrightarrow{\mathbf{G_0G_2}}$ as RM variables, and for $\delta\vec{\mathbf{r}}_{di}$ as DMC variables.

All vectors in the analysis were expressed in a global frame, with *X* in the anterior-posterior direction, *Y* vertical, and *Z* in the medio-lateral direction.

3. Results

Figure 4 shows an example of the decomposition of $\delta\vec{\mathbf{r}}_i$ in a specific instant. This figure reveals that nearly all the STA could be explained by a rigid movement of the marker cluster (see a video sample in Online Resource 1).

Table 1 shows the size of the RM and DMC components for each coordinate and for vector norms. The size of $\delta\vec{\mathbf{r}}_i$ was about three times the amplitude of bone

movement (3.35 mm/mm). The greatest value was in the direction of the applied vibration (3.05 mm/mm in *Y*-axis), although there were substantial relative movements in the other axes as well.

The RM component was over four times that of the DMC (3.22 mm/mm vs 0.71 mm/mm). Both components were substantially greater than the instrumental error (0.3 mm in absolute value, around 0.1 in the normalized scale) and greater than the clearance of the constrictions over the foot, ankle and knee (less than 1.0 mm in absolute value, 0.33 mm on the normalized scale).

The largest part of RM was a longitudinal translation of the marker cluster along the *Y*-axis, plus a small rotation (mean=1.40 deg/mm) around the medio-lateral axis (*Z*), compatible with the assumption of infinitesimal displacements. DMC was also greater in the *Y*-axis, although its size varied substantially across markers, so that the central ones underwent a smaller deformation. The measured STA rotation $d\boldsymbol{\theta}$ was substantially greater than the maximum angular error due to the potential motion of the tibia with respect to the frame (0.6 deg in absolute value, and 0.2 deg on the normalized scale).

Figure 5 shows the relationship between the RM variables and the phase variable q (vertical displacement of the tibia) for the subject #5. Both $\overrightarrow{\mathbf{G_0G}_2}$ and $d\vec{\boldsymbol{\theta}}$ show a small random dispersion around the functional average curves (small PIV), whereas the variability associated to such functional averages is proportionally much greater (high PDV). The average R coefficient, that represents the proportion between PDV and total variability was 0.992 for $\overrightarrow{\mathbf{G_0G}_2}$ (minimum 0.976), and 0.989 for $d\vec{\boldsymbol{\theta}}$ (minimum 0.974).

As already mentioned, $\delta\vec{\mathbf{r}}_{di}$ varied considerably across markers, so the PDV/PIV ratio was very variable as well. In general terms, DMC was more affected by PIV, although the *Y*-component tended to be greater and more correlated with q (see an example in Figure 6). The R coefficient depended on the marker: the interdecile range for individual markers was [0.60, 0.97], and the aggregated coefficient for all markers varied between 0.69 and 0.98 across subjects (average 0.87).

4. Discussion

Soft tissue artifacts are a major limitation in the analysis of human movement by videophotogrammetry. Previous studies show different approaches to the

assessment of STA, based on either the movement of individual markers in a bone-embedded frame or on the differences in results compared with an artifact-free standard. In this paper STA have been studied as the relative movement between the marker cluster as a single entity and the underlying bone. This approach is consistent with the usual practice of analyzing movement by adjusting marker coordinates to a rigid body movement, but it has been less studied in the literature. Fuller et al. [14] described the relative movement from the body's angular velocity, measured with a minimal set of 3 markers. There are also matrix methods for larger marker clusters, like the Point Cluster Technique and related variants, mentioned in the Introduction.

This paper proposes a vector method based on the composition of relative movements. Traditional methods based on the relative pose of technical and anatomical frames will yield the same results if the reference frame coincides with the anatomical frame in the initial position, but our proposal does not depend on the location of specific anatomical landmarks.

This representation has been used to analyze two aspects of STA: the quantification of RM and DMC, and the influence of bone movement on the variability of those components.

The quantification of the RM and DMC components is useful in some approaches to STA compensation. In effect, the isolation of the rigid component of STA is the basis of rigidization techniques for artifact compensation [2, 4, 10]. On the other hand, the deformation component has been used in noninvasive procedures to compensate for artifacts [6]. However, there are few studies that compare both components [30]. All these papers measure deformation as the variation in the eigenvalues of the marker inertia tensor. Another approach to modeling deformations is non-Euclidean transformations, as described in [11].

We have proposed a simple vector procedure to separate DMC and RM by decomposing marker displacements into a symmetric and a skew-symmetric field, respectively. This method does not require the calculation of eigenvalues, and the results represent the marker movements directly. Moreover, the equations in this procedure show that DMC is filtered and does not introduce kinematic errors if the rigid body condition is imposed in the analysis. This idea is supported by Stagni and Fantozzi's results, which imply that deformations are not good indicators of the RM component.

This study has also presented a model for quantifying the dependency between STA and bone movements, which is an important issue regarding the compensation techniques based on functional calibration [2,7-8, 16-17, 25, 29]. These techniques assume that there is a functional relation between bone movement and STA, so that the measured movement can be used to estimate the value of the artifact and eventually remove it. Therefore, their effectiveness depends on the part of the total variability that can be explained by such an estimation, although we have not found any work that performs such a quantification. That relation has been characterized by means of a nonlinear correlation coefficient, obtained from the functional average of a cyclical movement in the domain of the motion variable q. That coefficient quantifies the relative size of the systematic component of STA (PDV) vs. the total variability, when the functional relation with the phase variable q is nonlinear, as happens in this case.

In the experiment that has been reported (STA during sinusoidal motion of the shank with the knee flexed at 90 degrees, assuming no muscle tone), the artifact was essentially a rigid translation in the direction of the force applied to the leg, plus a small rotation around the medio-lateral axis. DMC was less than one quarter of the mean total artifact for individual markers. This agrees with the results in [31], and accounts for the limited effectiveness of the rigidization methods to compensate for STA [17].

With respect to the dependency between STA and bone movement, we have found slightly different behavior between the RM and DMC. The profile of $\overrightarrow{\mathbf{G_0G}_2}$ and $d\vec{\boldsymbol{\theta}}$ over the cycles was highly systematic, so the RM component was closely associated with the bone movement, in agreement with the results of previous studies [1, 16, 24-25]. DMC had a systematic part as well, but the influence of errors independent of the bone movement was relatively higher. This may be partly due to the smaller size of that component, but also to the fact that clusters with many markers (n=14 in our experiment) reduce the effect of random errors in the calculation of RM parameters [20], whereas there is no such reduction in the calculation of DMC variables.

The phase-dependent nature of STA has two important implications. On the one hand, it supports the strategy of multiple calibration based on STA models for specific movements, like the ones cited above. On the other hand, it calls into

question some validations of functional calibration methods based on simulations where the artifact has an important random component [11-13].

Extrapolations of these results must be done with caution, due to some limitations in the experiment performed. Most importantly, STA were elicited passively, without joint movements or muscular tension, and this departs from natural movements in clinical applications. Besides, the experiment was deliberately designed to obtain a substantial amplification of artifacts: a steady state of vibration around the resonant frequency of the soft tissue. These kinds of sinusoidal forces are quite different from the impacts which appear in gait, for instance, and can only be extrapolated to body vibrations. For instrumental reasons only shank artifacts have been measured, whereas the lower limb segment with the greatest STA is the thigh [17, 23]. It is possible that the application of this method to characterize STA in other body segments (e.g. the thigh) in natural movements (gait, sit-to-stand, etc.) with accurate measurement of the STA yield different relative sizes of the RM and DMC, and of their sources of variability. This may be confirmed in future studies using intracortical pins or fluoroscopy.

In the present study, instead of these gold standard procedures, the movement of the bone was obtained indirectly from the motion of a frame as rigidly as possible attached to the lower limb. Since this was not a direct observation of the bone, the possibility of some relative motion between the frame and the tibia cannot be rule out, although that possible additional artifact was controlled, and its estimated size was much smaller than the measured STA. On the other hand, this experimental setup had some advantages: it did not alter the movement of muscular tissues and was noninvasive and simple, so that it is possible to work with bigger subject samples than in other methods.

Regardless of the limitations associated with this specific experiment, the reported procedure for the kinematic characterization of STA can be applied for any other type of motion, just by using other experimental devices and phase variables.

All in all, this method contributes to improving our knowledge of STA by describing the part that affects the kinematic variables (RM), and by assessing the feasibility of estimating the value of STA on the basis of joint movements.

Acknowledgements

This work has been funded by the Spanish Government and co-financed by EU FEDER funds (Grants DPI2009-13830-C02-01, DPI2009-13830-C02-02 and IMPIVA IMDEEA/2012/ 79 and IMDEEA/2012/80).

References

1. Akbarshahi M, Schache AG, Fernandez JW, Baker R, Banks S, Pandy MG, (2010) Non-invasive assessment of soft-tissue artifact and its effect on knee joint kinematics during functional activity. J Biomech 43: 1292-1301
2. Alexander EJ, Andriacchi TP (2001) Correcting for deformation in skin-based marker systems. J Biomech 34: 355-361
3. Andersen MS, Benoit DL, Damsgaard M, Ramsey DK, Rasmussen J (2010) Do kinematic models reduce the effects of soft tissue artefacts in skin marker-based motion analysis? An in vivo study of knee kinematics. J Biomech 43: 268-273
4. Andriacchi TP, Alexander EJ, Toney MK, Dyrby C, Sum J (1998) A Point Cluster Method for In Vivo Motion Analysis: Applied to a Study of Knee Kinematics. J Biomech Eng 120: 743-749
5. Benoit DL, Ramsey DK, Lamontagne M, Xu L, Wretenberg P, Renström P (2006) Effect of skin movement artifact on knee kinematics during gait and cutting motions measured in vivo. Gait Posture 24: 152-164
6. Camomilla V, Donati M, Stagni R, Cappozzo A (2009) Non-invasive assessment of superficial soft tissue local displacement during movement: A feasibility study. J Biomech 42:931-937
7. Cappello A, Cappozzo A, La Palombara, PF, Lucchetti L, Leardini A (1997) Multiple anatomical landmark calibration for optimal bone pose estimation. Hum Mov Sci 16: 259-274
8. Cappello A, Stagni R, Fantozzi, S, Leardini, A (2005) Soft tissue artifact compensation in knee kinematics by double anatomical landmark calibration: performance of a novel method during select motor tasks. IEEE Trans Biomed Eng 52: 992-998

9. Cappozzo A, Della Croce U, Leardini A, Chiari L (2005) Human movement analysis using stereophotogrammetry: Part 1: theoretical background. Gait Posture 21: 186-196
10. Chèze L, Fregly BJ, Dimnet J (1995) A solidification procedure to facilitate kinematic analyses based on video system data. J Biomech 28: 879-884
11. Dumas R, Cheze L(2009) Soft tissue artifact compensation by linear 3D interpolation and approximation methods. J Biomech 42: 2214-2217
12. Ehrig RM, Taylor WR, Duda GN, Heller MO (2006) A survey of formal methods for determining the centre of rotation of ball joints. J Biomech 39: 2798-2809
13. Ehrig RM, Taylor, WR, Duda GN, Heller MO (2007) A survey of formal methods for determining functional joint axes. J Biomech 40: 2150-2157
14. Fuller J, Liu LJ, Murphy MC, Mann RW(1997) A comparison of lower-extremity skeletal kinematics measured using skin- and pin-mounted markers. Hum Mov Sci 16: 219-242
15. Gao B, Zheng N (2008) Investigation of soft tissue movement during level walking: Translations and rotations of skin markers. J Biomech 41: 3189-3195
16. Holden JP, Orsini JA, Siegel KL, Kepple TM., Gerber LH, Stanhope SJ (1997.) Surface movement errors in shank kinematics and knee kinetics during gait. Gait Posture 5: 217-227
17. Leardini A, Chiari L, Della Croce, U, Cappozzo A, 2005. Human movement analysis using stereophotogrammetry: Part 3. Soft tissue artifact assessment and compensation. Gait Posture 21: 212-225
18. Lucchetti L, Cappozzo A, Cappello A, Della Croce U (1998) Skin movement artefact assessment and compensation in the estimation of knee-joint kinematics. J Biomech 31: 977-984
19. Nester C, Jones RK, Liu A, Howard D, Lundberg A, Arndt A, Lundgren P, Stacoff A, Wolf P (2007) Foot kinematics during walking measured using bone and surface mounted markers. J Biomech 40: 3412-3423
20. Page A, de Rosario H, Mata V, Hoyos JV, Porcar R (2006) Effect of marker cluster design on the accuracy of human movement analysis using stereophotogrammetry. Med Biol Eng Comput 4: 1113-1119

21. Page A, de Rosario H, Mata V, Atienza C (2009) Experimental Analysis of Rigid Body Motion. A Vector Method to Determine Finite and Infinitesimal Displacements From Point Coordinates. J Mech Des 131: 031005
22. Page A, Galvez JA, de Rosario H, Mata V, Prat J (2010) Optimal average path of the instantaneous helical axis in planar motions with one functional degree of freedom. J Biomech 43: 375-378
23. Peters A, Galna B, Sangeux M, Morris M, Baker R (2010) Quantification of soft tissue artifact in lower limb human motion analysis: A systematic review. Gait Posture 31: 1-8
24. Reinschmidt C, van den Bogert AJ, Lundberg A, Nigg BM, Murphy N, Stacoff A, Stano A (1997) Tibiofemoral and tibiocalcaneal motion during walking: external vs. skeletal markers. Gait Posture 6: 98-109
25. Ryu T, Choi HS, Chung MK. (2009) Soft tissue artifact compensation using displacement dependency between anatomical landmarks and skin markers- a preliminary study. Int J Ind Ergon 39: 152-158
26. Sangeux M, Marin F, Charleux F, Dürselen L, Ho Ba Tho M C (2006) Quantification of the 3D relative movement of external marker sets vs. bones based on magnetic resonance imaging. Clin Biomech 21: 984-991
27. Sati, M., de Guise, J. A., Larouche, S., Drouin, G., 1996. Quantitative assessment of skin-bone movement at the knee. The Knee, 3(3), 121-138.
28. Stagni, R., Fantozzi, S., Cappello, A., Leardini, A., 2005. Quantification of soft tissue artefact in motion analysis by combining 3D fluoroscopy and stereophotogrammetry: a study on two subjects. Clin Biomech, 20(3), 320-329.
29. Stagni, R., Fantozzi, S., Cappello, A. , 2009. Double calibration vs global optimization: performance and effectiveness for clinical application. Gait Posture, 29, 119-122.
30. Stagni, R., Fantozzi, S., 2009. Can cluster deformation be an indicator of soft tissue artefact? Gait Posture, 30(Supplement 1), S55.
31. Taylor, W. R., Ehrig, R. M., Duda, G. N., Schell, H., Seebeck, P., Heller, M. O., 2005. On the influence of soft tissue coverage in the determination of bone kinematics using skin markers. J Orthop Res, 23(4), 726-734.
32. Tranberg, R., Karlsson, D., 1998. The relative skin movement of the foot: a 2-D roentgen photogrammetry study. Clin Biomech, 13(1), 71-76.

33. Tsai, T.-Y., Lu, Tung-Wu, Kuo, M.-Y., Lin, C.-C., 2011. Effects of soft tissue artifacts on the calculated kinematics and kinetics of the knee during stair-ascent. J Biomech, 44(6), 1182-1188.
34. Woltring, H. J., Long, K., Osterbauer, P. J., and Fuhr, A. W., 1994. "Instantaneous Helical Axis Estimation From 3-D Video Data in Neck Kinematics for Whiplash Diagnostics," J. Biomech, 27(12), 1415–1432.

FIGURE CAPTIONS

Figure 1 Bone displacement is defined by $\{\vec{\theta}; \overrightarrow{\mathbf{G}_0\mathbf{G}_1}\}$, so that a point P_{i0} would move to P_{i1}, but skin markers experience a superimposed displacement with respect to the bone $\delta\vec{\mathbf{r}}_i'$, and the observed position of the point is P_i. The relative movement of the markers, $\delta\vec{\mathbf{r}}_i$, is calculated by applying the opposite displacement $\{-\vec{\theta}; -\overrightarrow{\mathbf{G}_0\mathbf{G}_1}\}$. Therefore, P_i moves back to P_{i2}, and $\delta\vec{\mathbf{r}}_i$ is the vector that goes from P_{i0} to that point.

Figure 2 (a) A synthetic example of decomposition of a field of infinitesimal displacements (black arrows) into two components: skew-symmetric component (grey thick arrows) and symmetric component (grey thin arrows). (b) The skew-symmetric field corresponds to the rigid motion: it is equivalent to a displacement and a rotation. (c) The symmetric component is the deformation field. This field does not imply any global motion, because both the rotation and the displacement of its centre are null. Therefore, for any kinematic analysis procedure that works with Euclidean transformations (rigid condition), the measured motion of (a) is the same as that measured in (b).

Figure 3 Experimental setup. The rigid metallic frame is fixed to the vibration exciter. The subject's leg is firmly attached to the frame by the foot support and two rigid structures are pressed against the malleoli and epycondiles. Moreover, the top horizontal bar is pressing down on the knee to prevent vertical movements between the frame and the tibia

Figure 4 Example of relative displacement fields of the markers (subject #5). Black vectors represent the total displacement $\delta\vec{\mathbf{r}}_i$; grey, short vectors ending in circles are the symmetric field ($\delta\vec{\mathbf{r}}_{di}$); grey, without end markers are the skew-symmetric field ($\delta\vec{\mathbf{r}}_{si}$)

Figure 5 Phase diagrams of the rigid motion associated to the STA. a) Marker centroid displacement $\overrightarrow{\mathbf{G}_0\mathbf{G}_2}$; b) cluster rotation $d\bar{\boldsymbol{\theta}}$, for subject #5. Points represent the measured values, and the "fitted" curves represent the functional averages across cycles ($\overrightarrow{\mathbf{G}_0\mathbf{G}_2}(q)$ and $d\bar{\boldsymbol{\theta}}(q)$, respectively).

Figure 6 Phase diagram of the DMC component of marker #4 ($\delta\tilde{\mathbf{r}}_{d4}$) for subject #5. Points represent the measured values, and the "fitted" curves represent the functional average across cycles, $\delta\tilde{\mathbf{r}}_{d4}(q)$.

Online Resource 1. Video sample.

Figure 1
Click here to download high resolution image

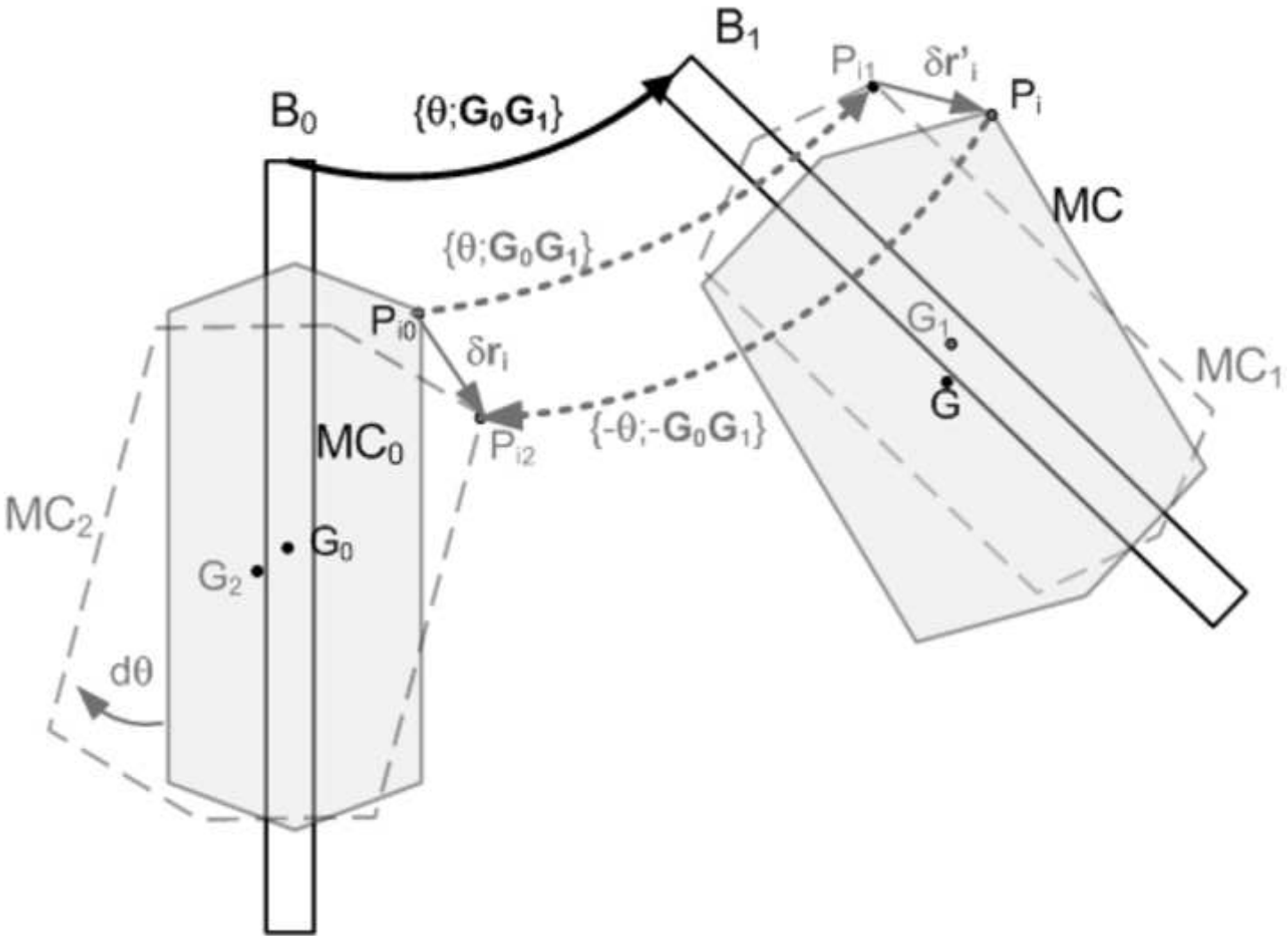

Figure 2
Click here to download high resolution image

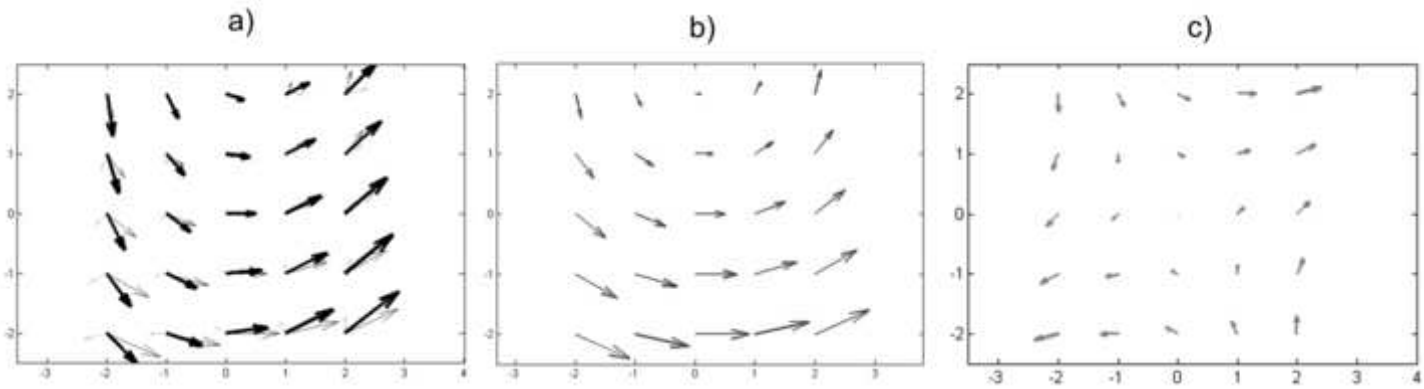

Figure 3
Click here to download high resolution image

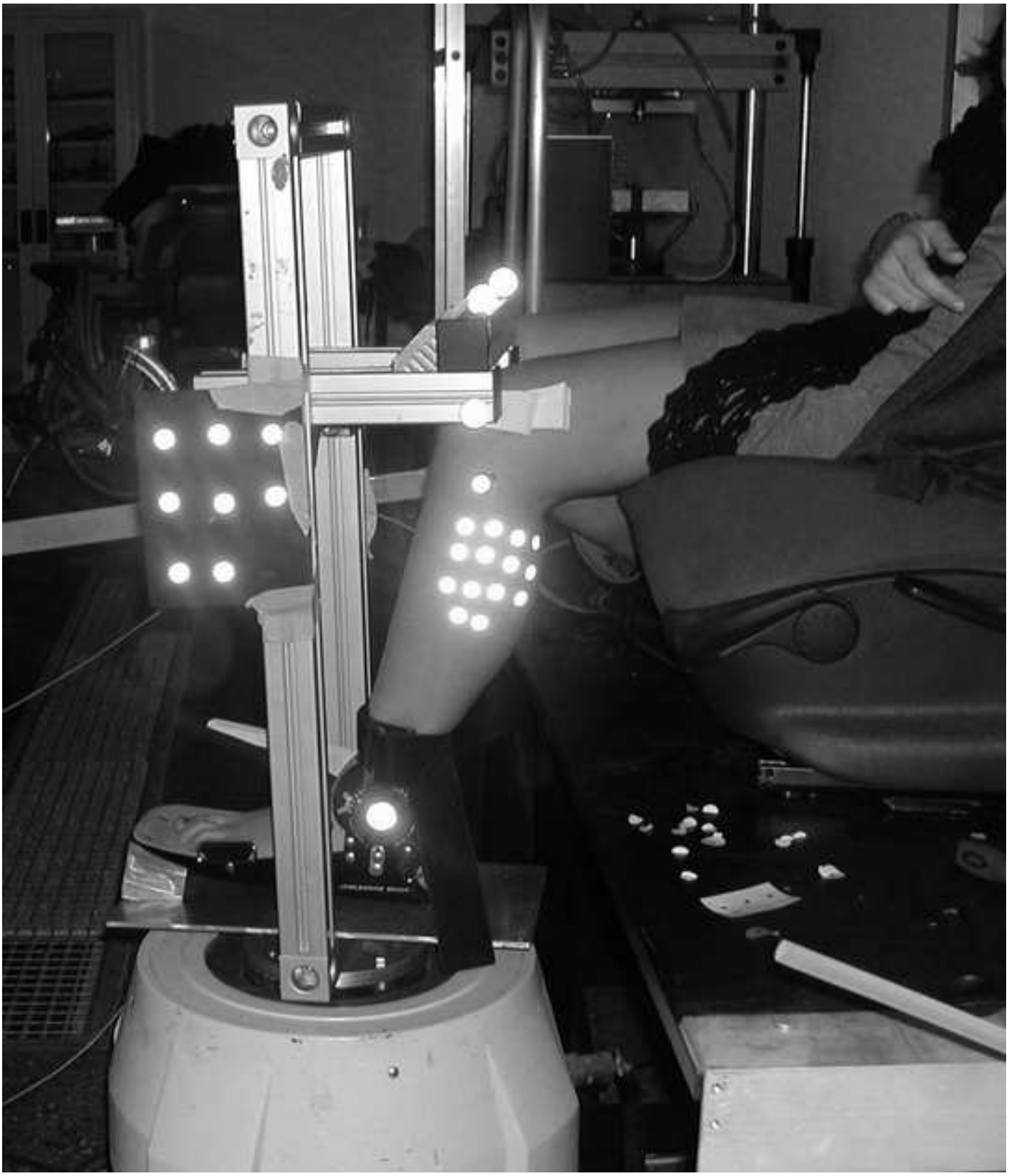

Figure 4
Click here to download Figure: Figure 4.eps

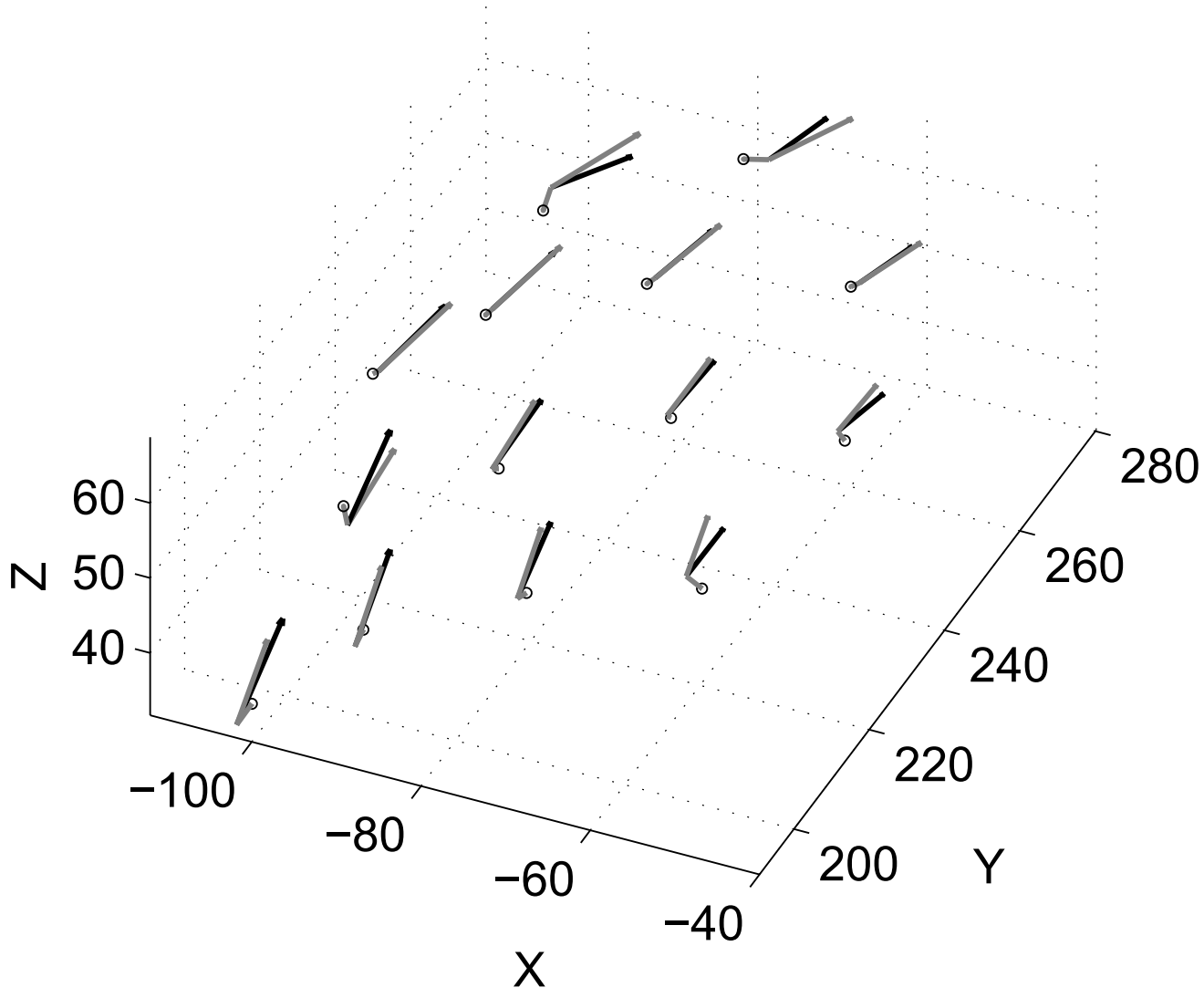

Figure 5a
Click here to download Figure: Figure 5a.eps

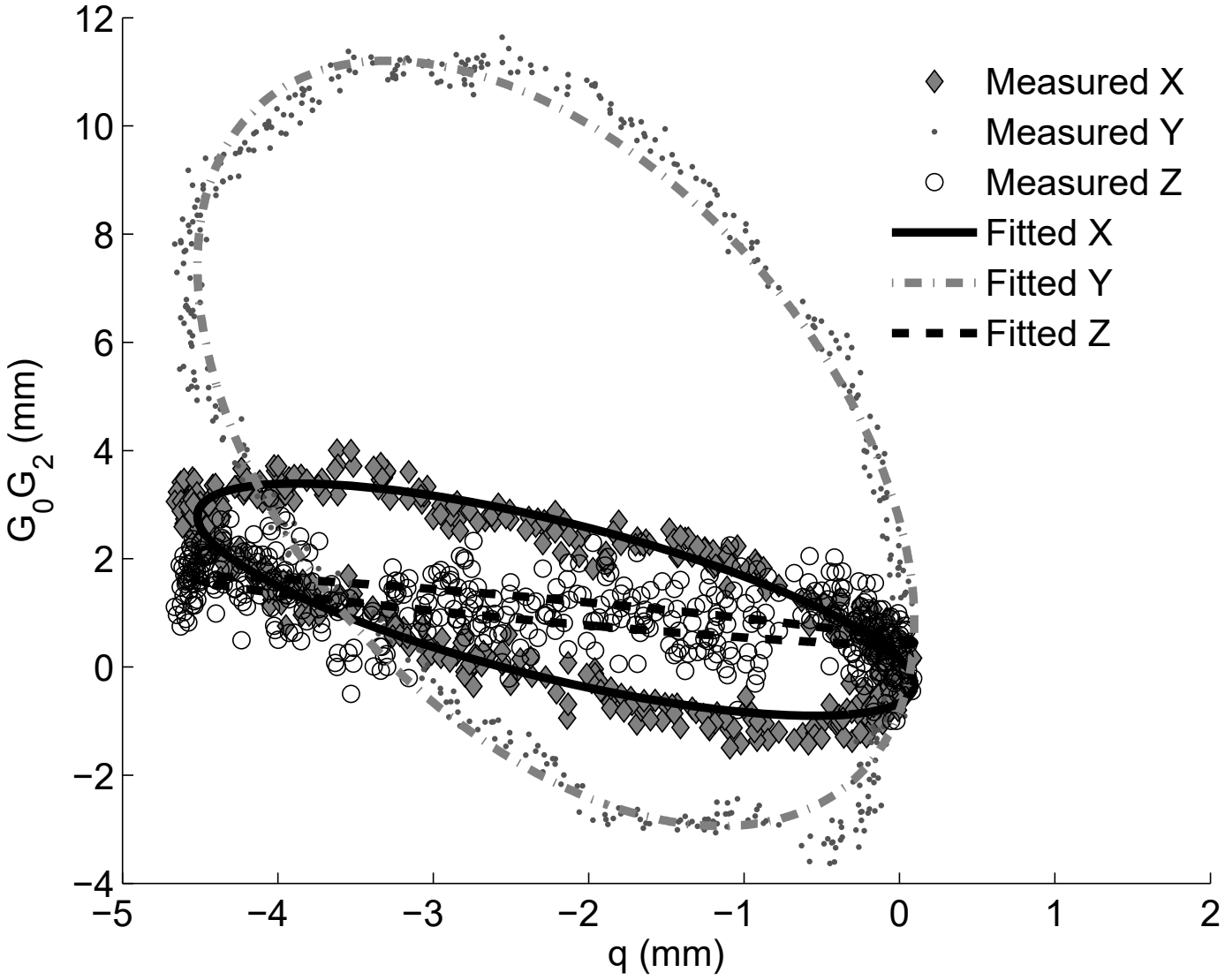

Figure 5b
Click here to download Figure: fig 5b.eps

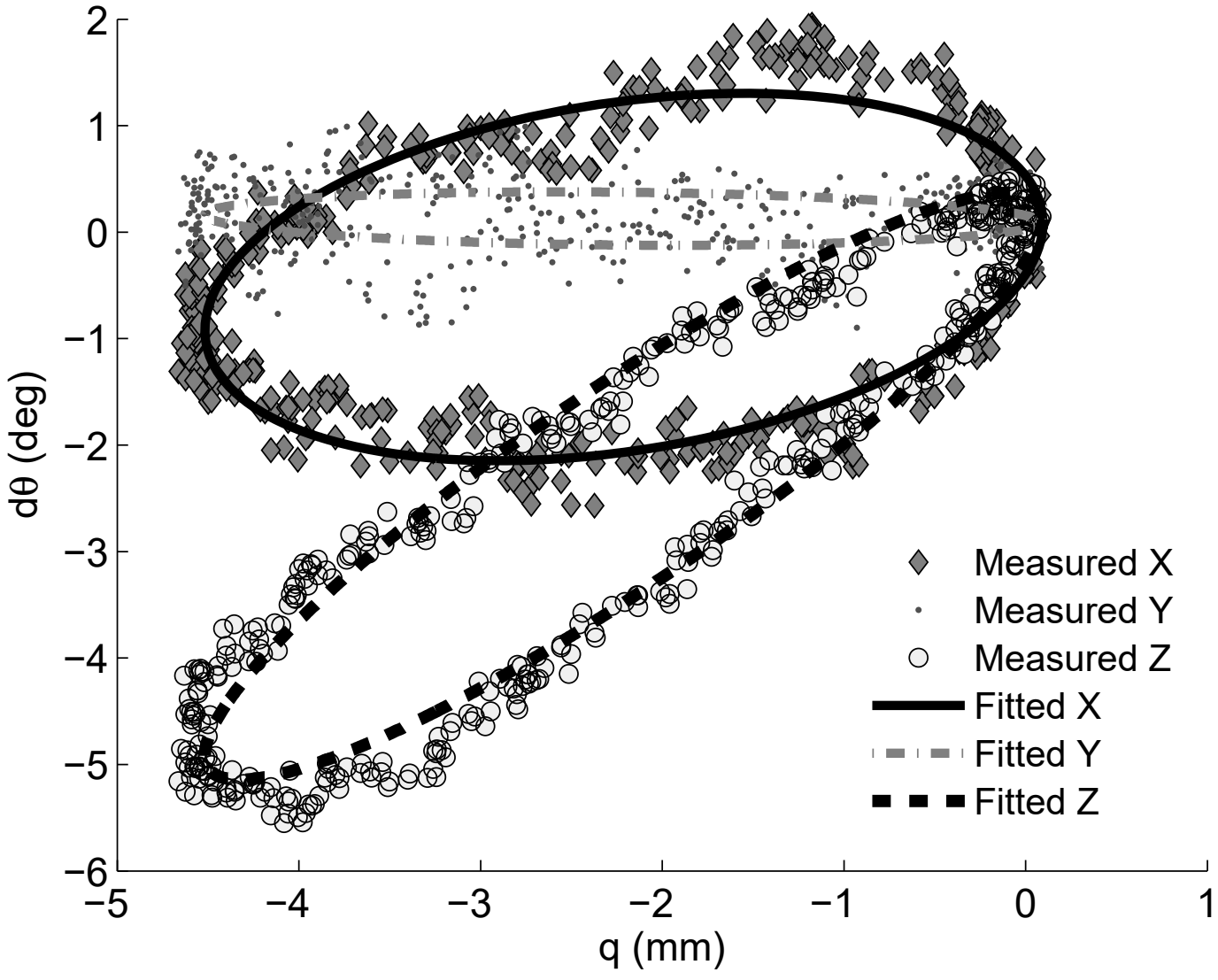

Figure 6
Click here to download Figure: marc4.eps

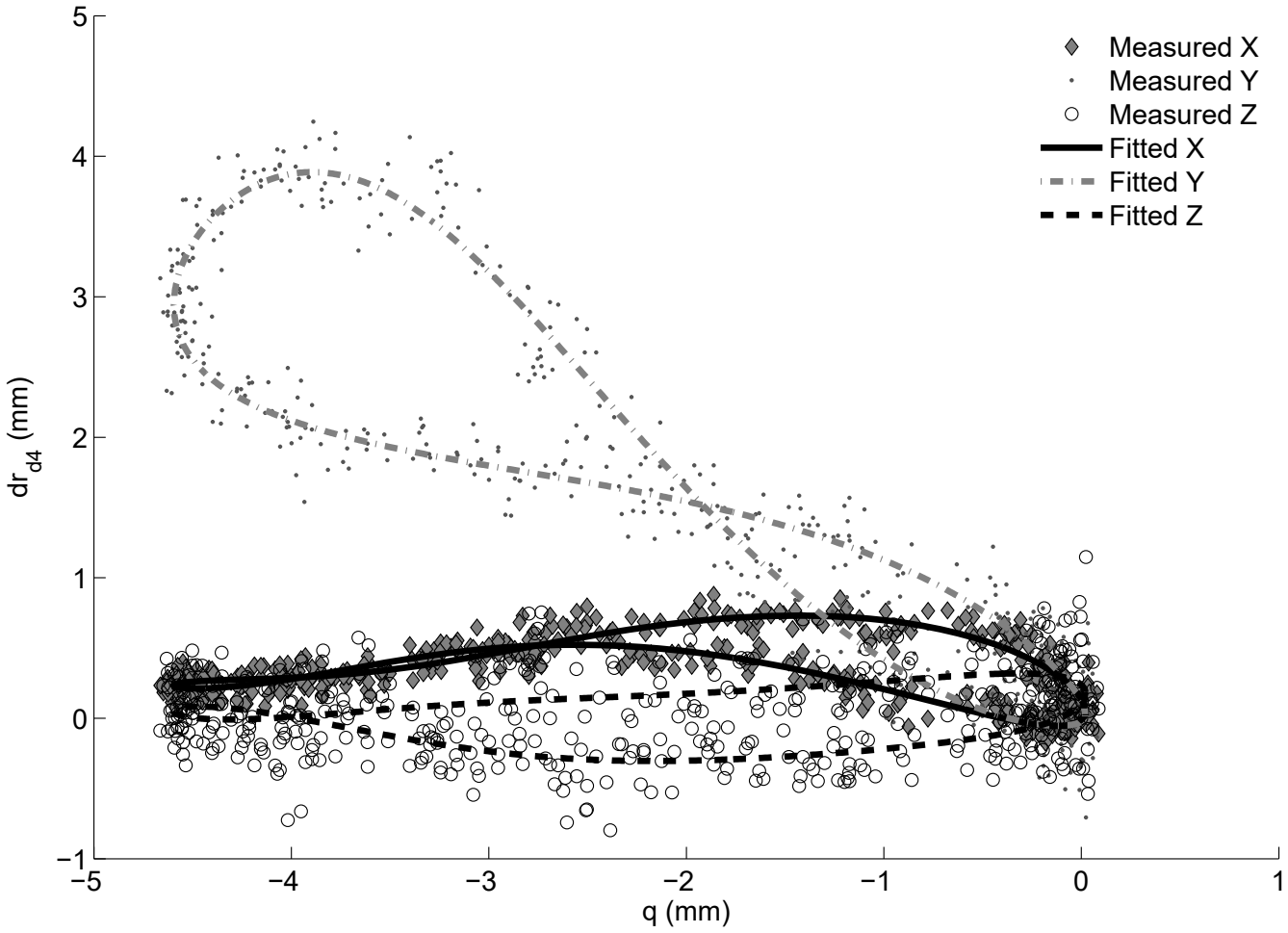

table 1
Click here to download table: Table 1.doc

Table 1

RMS averages and standard deviations for RM and DMC variables. All values are normalized with respect to the peak-to-peak amplitude of the vertical bone movement.

Component	**Variable**	**X coordinate**	**Y coordinate**	**Z coordinate**	**Norm**
Total STA	$\delta\vec{\mathbf{r}}_i$ (mm/mm)	0.88 (0.33)	3.05 (0.80)	0.92 (0.28)	3.35 (0.79)
DMC	$\delta\vec{\mathbf{r}}_{di}$ (mm/mm)	0.34 (0.13)	0.46 (0.16)	0.41 (0.13)	0.71 (0.24)
RM	$\delta\vec{\mathbf{r}}_{si}$ (mm/mm)	0.91 (0.31)	3.00 (0.81)	0.83 (0.29)	3.22 (0.78)
	$\overrightarrow{\mathbf{G_0G_2}}$ (mm/mm)	0.73 (0.27)	2.96 (0.82)	0.73 (0.31)	3.09 (0.85)
	$d\vec{\boldsymbol{\theta}}$ (deg/mm)	0.77 (0.25)	0.63 (0.23)	1.40 (0.52)	1.72 (0.60)

Video Sample

Click here to download Supplementary material (videos/animations/long tables): suppl.gif